Available online at www.CivileJournal.org

Civil Engineering Journal

Vol. 6, No. 6, June, 2020

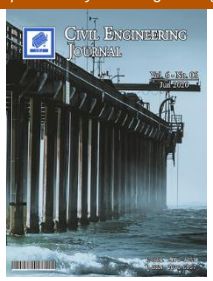

Sacrificial Piles as Scour Countermeasures in River Bridges A Numerical Study using *FLOW-3D*

Mohammad Nazari-Sharabian [a*], Aliasghar Nazari-Sharabian [b], Moses Karakouzian [a], Mehrdad Karami [c]

[a] *Department of Civil and Environmental Engineering and Construction, University of Nevada, Las Vegas, Las Vegas, NV 89154, USA.*

[b] *Department of Civil and Architectural Engineering, Parsian Higher Education Institute, Ghazvin 3414896818, Iran.*

[c] *Department of Civil Engineering, Isfahan University of Technology, Isfahan 8415683111, Iran.*

Received 13 December 2019; Accepted 10 April 2020

Abstract

Scour is defined as the erosive action of flowing water, as well as the excavating and carrying away materials from beds and banks of streams, and from the vicinity of bridge foundations, which is one of the main causes of river bridge failures. In the present study, implementing a numerical approach, and using the *FLOW-3D* model that works based on the finite volume method (FVM), the applicability of using sacrificial piles in different configurations in front of a bridge pier as countermeasures against scouring is investigated. In this regard, the numerical model was calibrated based on an experimental study on scouring around an unprotected circular river bridge pier. In simulations, the bridge pier and sacrificial piles were circular, and the riverbed was sandy. In all scenarios, the flow rate was constant and equal to 45 L/s. Furthermore, one to five sacrificial piles were placed in front of the pier in different locations for each scenario. Implementation of the sacrificial piles proved to be effective in substantially reducing the scour depths. The results showed that although scouring occurred in the entire area around the pier, the maximum and minimum scour depths were observed on the sides (using three sacrificial piles located upstream, at three and five times the pier diameter) and in the back (using five sacrificial piles located upstream, at four, six, and eight times the pier diameter) of the pier. Moreover, among scenarios where single piles were installed in front of the pier, installing them at a distance of five times the pier diameter was more effective in reducing scour depths. For other scenarios, in which three piles and five piles were installed, distances of six and four times the pier diameter for the three piles scenario, and four, six, and eight times the pier diameter for the five piles scenario were most effective.

Keywords: Scouring; River Bridges; Sacrificial Piles; Finite Volume Method (FVM); *FLOW-3D*.

1. Introduction

Bridges are important structures commonly constructed on rivers and in valleys for the purpose of vehicular traffic access [1]. Despite extensive progress in structural and hydraulic engineering [2, 3], bridge failures and other vulnerabilities, observed globally, continue to result in economic loss, social problems, and human casualties [4]. One major hazard that bridges are subjected to is local scouring around piers [5]. Bridge piers located in a river's path lead to a reduction of the river's cross-section. This situation leads to increased flow velocity around piers, and as a result, the deviation of the flow lines toward the bed forms a horseshoe vortex, as well as rotary and uprising flows. The shearing forces originating from the flow in the riverbed increase with increasing water velocity. By overcoming the

* Corresponding author: nazarish@unlv.nevada.edu

http://dx.doi.org/10.28991/cej-2020-03091531

resistant shear forces of the bed, these active forces cause the suspension and movement of the river bed materials. If the flow is strong enough, it penetrates into the depth of the riverbed over time, and if it reaches below the bridge's foundations, the bearing capacity of the soil decreases significantly. Consequently, the foundations settle and eventually the bridge collapses [6]. Figure 1 shows a simplified mechanism of the local scour around a bridge pier.

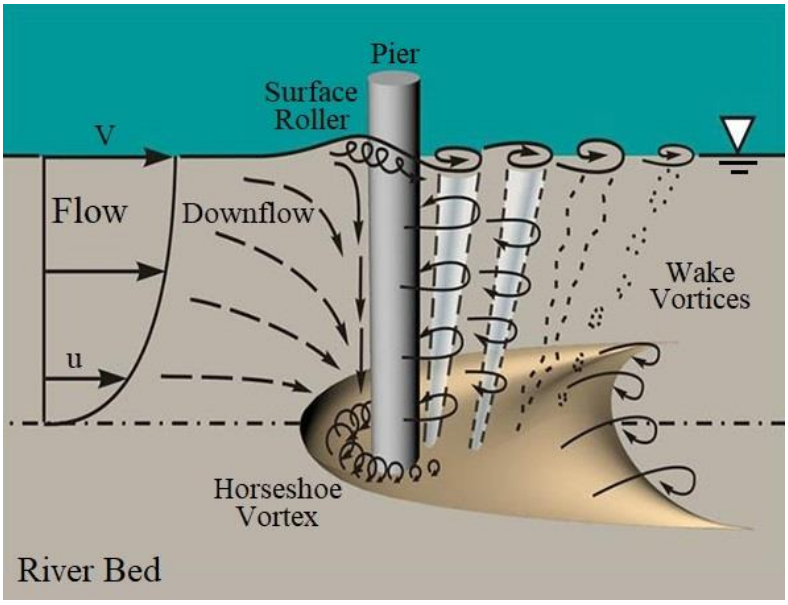

Figure 1. Simplified scouring mechanism around a bridge pier [7]

According to the literature, Chiew proposed two methods to reduce scouring around bridge piers. The first method was using a slot in the bridge pier in order to divert the flow away from the riverbed. The second method was placing a collar around the pier to reform the flow patterns around it. The author concluded that a combination of slot and collar methods can substantially reduce scouring [4]. In another study, performing experiments on cylindrical piers in clear-water conditions with uniform sandy beds, Richardson and Davis obtained a formula based on the ratio of the length to width of the pier, and the approach angle of flow to the pier [6]. The equation they obtained predicts maximum local pier scour depth (Equation 1).

$$\frac{y_s}{y_1} = 2.k_1.k_2.k_3.k_4\left(\frac{a}{y_1}\right)^{0.65} Fr_1^{0.43} \quad (1)$$

Where the scour depth is represented by y_s (m); y_1 is the flow depth directly upstream of the pier (m); k_1 is the shape correction factor for the pier nose; k_2 is the correction factor for the flow angle of attack; k_3 is the correction factor for the bed condition; k_4 is the correction factor for armoring by bed material size; the pier width is represented by a (m); and Fr_1 is the Froude number directly upstream of the pier. In addition, the correction factor, k_2, for the flow angle of attack, θ, is calculated using the following equation:

$$k_2 = (cos\,\theta + \frac{L}{a}\,sin\,\theta)^{0.65} \quad (2)$$

Where L is the pier length. If D_{50} < 2 mm or D_{95} < 20 mm, then k_4 = 1. k_1 and k_3 are determined from Table 1. Richardson and Davis calculated the scour depth based on the ratio of length to width of the pier using the k_2 factor (Figure 2).

Table 1. k_1 and k_3 values based on the shape of the pier nose and the dune height

The shape of the pier nose	k_1	Bed condition	Dune height (m)	k_3
Square nose	1.1	Clear-water scour	-	1.1
Round nose	1	Plane bed and antidune flow	-	1.1
Circular cylinder	1	Small dunes	0.6 ≤ H < 3	1.1
Group of cylinders	1	Medium dunes	3 ≤ H < 9	1.1 to 1.2
Sharp nose	0.9	Large dunes	9 ≤ H	1.3

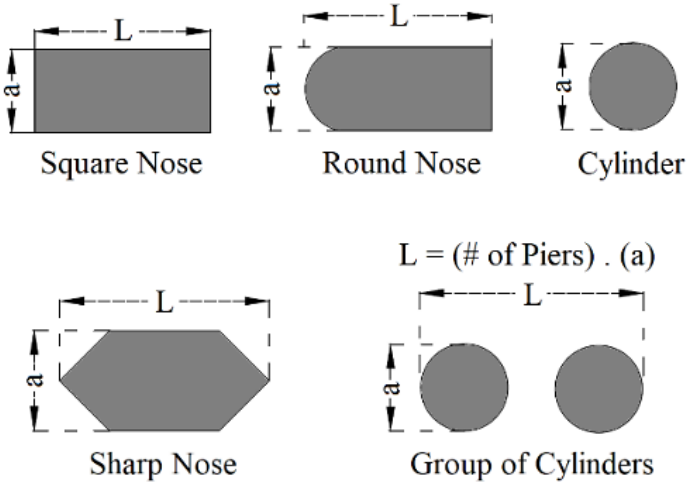

Figure 2. Pier shapes studied by Richardson and Davis [6]

Moreover, Chang et al. (2004) conducted experiments on the scour depth around cylindrical piers in clear-water conditions, using uniform sediment for the bed. The authors provided a regression model based on the pier's diameter and the average size of the bed's sediment particles [8]. Unger and Hager used ripraps in three levels relative to the channel bed (at equal height, higher than, and lower than the bed), to investigate the reduction in scour depth. The authors concluded that the minimum scour depth occurred when the ripraps were installed at the same level as the river bed [9]. Abdeldayem et al. investigated the effect of installing a group of sacrificial piles in front of bridge piers, in different configurations, as a countermeasure against scouring. The authors concluded that the method was effective in reducing the scour depth [10]. In another study, and based on the concept of effective pier width, which was a relationship between the shape factor and width of the pier, Sheppard et al. provided a relationship for estimating the scour depth [11]. Melville and Hadfield performed experimental studies on the impact of using sacrificial piles as pier scour countermeasures. They concluded that sacrificial piles are less effective under live-bed conditions, due to the passage of bed forms. However, their implementation is recommended as far as the flow remains aligned, and the flow intensity is relatively small [12]. Furthermore, Yao et al. performed an experimental investigation on local scouring around sacrificial bridge piers with circular and square cross-sections. The authors demonstrated that the equilibrium scour depth for square piers was generally larger than that for circular piers [13].

More recently, Link et al. analyzed bridge pier scouring during flood waves. The waves were created in a novel installation that was able to produce complex and accurate hydrographs. The authors reported the impact of different hydrographs on scouring, and demonstrated strong control by the hydrograph shape of the temporal evolutions of scour depth and scouring rate. Moreover, they concluded that in the process of scouring, flow acceleration plays a minor role [14]. In an experimental study, Khan et al. investigated the scouring patterns in a lateral direction for circular and square pier models. They reported that the pier scour depth and the affected area around pier increase with an increase in pier size. Moreover, the square pier models resulted in greater scour depths and areas, as compared to circular pier models [15]. Moreover, in another experimental study by Yang et al., local scour at complex bridge piers were investigated in clear-water conditions. Two typical pier models, nine pile-cap elevations and seven pier skew angles, were used. The pier was skewed from 0° to 90° with 15° intervals. Based on the skewness of the pier, three categories of aligned pier (= 0°), slightly skewed pier ($\alpha \approx 15°$), and highly skewed pier ($\alpha \geq 30°$) were defined. The authors concluded that a slight skew angle can significantly increase the equilibrium scour depth. Moreover, as the α increased, the influences of the pile cap and the pile group on the scouring process were weakened. Finally, the authors presented a new scour prediction model which led to a higher safety margin [16]. Moussa et al. performed experimental and numerical studies on the local scour depth at bridge supports. They implemented a computational fluid dynamic model (SSIIM), to simulate scouring around bridge supports. They found that the existence of debris and industrial wastes leads to an increase in the local scour depth around bridge foundations, and the scour depth depends on the Froude number and dimensions of the obstacle. Finally, they proposed empirical equations for estimating local scour depths at bridge supports based on multiple linear regressions [17].

Furthermore, Guan et al. used Particle Image Velocimetry (PIV) to study the detailed turbulent flow field in a developing clear-water scour hole around a circular pier. The authors reported that the horseshoe vortex system evolved from one initially small vortex to three vortices during the scour development. Moreover, by increasing the scour depth, the strength and size of the main vortex increased as well. At a location upstream of the main vortex, regions of both maximum turbulence intensity and Reynolds shear stress were formed [18]. Dougherty used the Reynolds-Averaged Navier–Stokes (RANS) equations, with k–ω and k-ε turbulence closure models, to model the

hydrodynamic component of local scour around a circular pier. Afterward, for a Reynolds number of 1.7×10^5, they used the k-ε model for the following circular pier attachments – tapered streamlined sheath, delta vane, guide wall with slanting plates, and angled plate footings – in order to predict bed shear stress and velocity distribution profiles. The results indicated that compared to the circular pier, the reduction in simulated maximum bed shear stress was 30% for the delta vane and angled plate footings, 20% for the tapered streamlined sheath, and 15% for the guide wall with slanting plates. The delta vane was then compared to the circular pier for a Reynolds number of 5.1×10^6, in which the reduction in maximum bed shear stress was 22%. Finally, they concluded that by reducing the bed shear stress, these pier configurations have the ability to reduce the scour potential by altering the flow near the pier [19].

In an experimental study, Vijayasree et al. (2017) investigated the local scour around bridge piers of different shapes (rectangular, oblong, trapezoidal, triangular and lenticular) on a sediment bed. They used a 3D Micro-acoustic Doppler Velocimeter (ADV) to record the instantaneous velocity data for five different discharges. They found that at the leading edge of the rectangular pier, the upstream scour depth was maximum, and at the same location, it was minimum for the lenticular pier [20].

Moreover, to reduce the flow stagnation and vortex formation in front of a bridge pier, Farooq and Ghumman performed an experimental study using a collar, hooked collar, cable, and openings, separately and in combination, around a pier. Six different pier shapes were used to determine the influence of pier shape on local scouring, for a length-width ratio smaller than or equal to three. Among the pier shapes studied, a plain octagonal shape had more satisfactory results in reducing the scour depth. Furthermore, for the octagonal bridge pier, the efficiency of pier modification was evaluated by testing different combinations of collar, hooked collar, cable, and openings. The results showed that the scour depth was reduced significantly by applying these modifications. The best combination was found to be a hooked collar with cable and openings, which reduced almost 53% of the scour depth [21].

Furthermore, in order to investigate the effects of different flow and sediment regimes during flood waves, Link analyzed the local scour and sediment deposition at a bridge pier. They performed field measurements of scouring and streamflow during six days, at the Rapel Bridge, located over the Rapel River in Central Chile. The authors then proposed a simple mathematical model of scouring and deposition. Considering different excess sediment supplies, they applied the model to pre- and post-dam scenarios to compare the expected scouring caused by a natural flow regime and by hydropeaking. The model application showed that scouring and deposition were very sensitive to the excess sediment supply [22].

The literature review showed that researchers have proposed different countermeasures for protecting bridges against scouring. For instance, many flow-altering scour countermeasures were studied, including altering the geometry of the pier itself, or adding a sheath or a plate to the base of the pier. However, none of the studies investigated using sacrificial piles in arrangements as scour countermeasures upstream of a pier, as in the present study. Moreover, most of these studies were performed experimentally. Considering the limitations and costs of setting up laboratory experiments, a numerical modeling approach was implemented in this study. In this regard, using the *FLOW-3D* model, the applicability of diverse arrangements and different numbers of sacrificial piles in front of a circular pier for reducing the scour depth around the pier was investigated. The following flowchart presents the methodology employed in the present study.

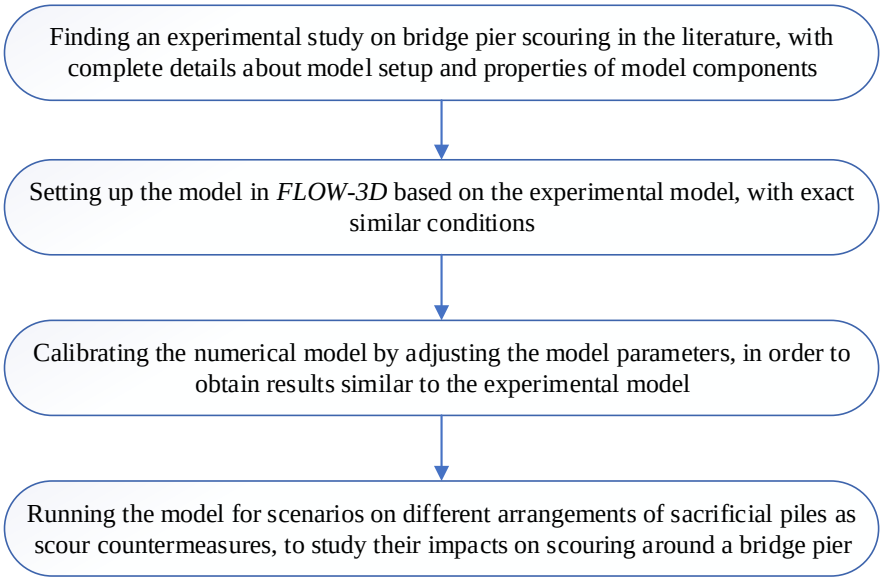

Figure 3. Flowchart of the present study

2. Materials and Methods

2.1. *FLOW-3D* Model

In different fields of science and engineering, computer simulations are being used for the mathematical modeling of many natural systems. When analytical solutions are too complex, simulations can be used to estimate the performance of systems [23]. Several software packages are available for fluid flow analysis. Among these packages, selecting a suitable one is a challenging proposition, considering their physical approximations and numerical solution techniques. *FLOW-3D* is computational fluid dynamics (CFD) software, which solves the equations of motion in multi-scale, multi-physics flow problems. Considering its capabilities, users can apply *FLOW-3D* to a wide variety of fluid flow phenomena [24].

FLOW-3D works on the basis of the finite-volume method to solve fluid dynamics equations. In this method, by employing the divergence theorem in a partial differential equation, volume integrals that contain a divergence term are converted to surface integrals. Afterward, these terms are evaluated as fluxes at the surfaces of each finite volume. More details on *FLOW-3D* model theory, such as meshing and geometry, fluid dynamics equations, implicitness and accuracy, relaxation and convergence parameters, free-surface tracking, etc., can be found in the *FLOW-3D* user manual [24].

2.2. Sediment Scour Model in *FLOW-3D*

In *FLOW-3D*, the sediment scour model simulates the movement of the packed and suspended sediment. This movement causes erosion around bridge foundations. As described by Brethour [25], this model has drifting and lifting modules. The driving force that suspends the sediment particles is produced by the drifting module. Local bed shear stress separates the particles from the sediment bed, and is applied by the lifting module. Moreover, the drag model controls the sediment behavior. The drag model is activated when the sediment concentration exceeds a cohesive solid fraction defined by the user. The suspended and packed sediment constitute the distribution of sediment in the flow field in *FLOW-3D*. As the concentration of the suspended sediment increases, the fluid viscosity increases. The solid-like behavior is predicted by an additional linear drag term to the momentum equation, *-Ku*, as follows [26]:

$$\frac{\partial u}{\partial t} + u.\nabla u = -\nabla P/\overline{\rho} + \nabla.\tau/\overline{\rho} + g - Ku \quad (3)$$

$$\overline{\rho} = \rho_l + f_s(\rho_s - \rho_l) \quad (4)$$

Where $\bar{\rho}$ represents the average density on the packed sediment bed; local density of liquid and sediment particles are represented by ρ_l and ρ_s, respectively; τ is the shear stress due to the fluid viscosity; and, K is the drag coefficient among particles. Based on the assumptions of the solid-like behavior, K can be calculated using the following formula [26]:

$$K = \begin{cases} 0 & f_s < f_{s,co} \\ \left(\frac{f_{s,cr} - f_{s,co}}{f_{s,cr} - f_s}\right)\left(\frac{f_{s,cr} - f_{s,co}}{f_{s,cr} - f_s} - 1\right) & f_{s,co} < f_s < f_{s,cr} \\ \infty & f_{s,cr} < f_s \end{cases} \quad (5)$$

Where the solid fraction of the sediment is represented by f_s; $f_{s,co}$ is the cohesive solid fraction (when the interaction among particles occurs and fluid viscosity does not increase with the sediment concentration); and $f_{s,cr}$ is the critical solid fraction (when the fluid flow ceases and behaves as a solid mass). Moreover, u_{drift} and u_{lift} are the two components of the local velocity vectors of particles, and are modeled by the following equations [26]:

$$u_{drift} = \frac{f_l d^2}{18\mu}\frac{\nabla P}{\overline{\rho}}(\rho_s - \rho_l) \quad (6)$$

$$u_{lift} = \alpha n_s \sqrt{\frac{\tau - \tau_{crit}}{\overline{\rho}}} \quad (7)$$

Where d is the mean sediment diameter; f_l is the liquid fraction; and μ is the liquid viscosity, which can be calculated using [26]:

$$\mu = \mu_l\left(1 - \frac{min(f_s, f_{s,co})}{f_{s,cr}}\right)^{-1.55} \quad (8)$$

Where the molecular viscosity of the liquid is represented by μ_l. Equation 6 states that as the solid fraction, or sediment concentration, increase the average viscosity of the fluid will increase. This continues to happen until the solid fraction and the cohesive solid fraction are equal. At this point, the solid-like model activates, and the fluid viscosity cannot increase. When the critical solid fraction is equal to the solid fraction, the fluid viscosity becomes infinite. This means that, identical to the model of the drag coefficient, the complete status of solid forms. Additionally, in the regions of $f_l = 0$, u_{drift} becomes zero; the probability of a particle's lifting from the packed sediment surface is represented by α ($0 < \alpha < 1$); n_s is the normal vector to the bed surface; and τ_{crit} is the stress required to friction the particle away from the packed sediment interface (critical shear stress), and is modeled by the critical Shields number (Equation 9). The dimensionless Shields number is constructed as the ratio between the shear stress at the top of the particle bed and the apparent weight of a single particle [26].

$$\theta_{crit} = \frac{\tau_{crit}}{g(\rho_s - \rho_l)d} \tag{9}$$

An assumption in the drifting model is that the transport of most of the sediment particles away from the packed bed interface is dominated by suspension and advection. The scour is a function of the shear stress of fluid at the bed level, critical shear stress that starts the erosion, and the density difference between the fluid and solid particles. Moreover, the bed-load movement is simulated by the lifting model, which also predicts the local flux of sediment eroded on the packed bed interface. Generally, when the normalized bed shear stress is higher than the critical value, sediment flux occurs. The angle of repose in the sediment erosion model of *FLOW-3D* can be defined by the user. Based on the following equation, the critical shear stress is dependent on the ratio of the actual slope to the angle of repose [26]:

$$\tau_{crit} = \tau_{crit}^{0}\sqrt{1 - \frac{sin^2\,\phi}{sin^2\,\omega}} \tag{10}$$

Where the critical shear stress on the packed sediment bed with a slope is represented by τ_{crit}; in a horizontal bed, τ_{crit}^{0} is the critical shear stress; Φ is the actual angle between the normal vector of the bed interface and the gravity vector; and ω is the angle of repose. When $\varphi = \omega$, τ_{crit} (the locally critical shear stress) is equal to zero. This means that the sediment particles will slide along the slope in case of any disturbance from the flow region; the locally critical shear stress will be restored to the critical value with the horizontal slope when $\varphi = 0$. To model the motion of the suspended sediment in the flow domain in *FLOW-3D*, the advection-diffusion equation is employed as follows [26]:

$$(\frac{\partial C_s}{\partial t})_x + u.\nabla C_s = D\nabla^2 C_s - u_{lift}.\nabla C_s - u_{drift}.\nabla C_s \tag{11}$$

In which the local velocity of advection is represented by u; C_s is the local concentration of the suspended sediment; and D is the diffusion coefficient. In the advection-diffusion equation, two additional items originate from the influence of the drifting and lifting of the sediment. In the region where the local shear stress cannot exceed the critical value (τ_{crit}), u_{lift} is zero. Therefore, in most of the flow domains, there is no influence of lifting on the motion of the suspended sediment, and it only occurs in the vicinity of the packed sediment interfaces.

2.3. Model Setup and Calibration

2.3.1. Experimental Model

The numerical model was calibrated based on an experiment performed by Balouchi and Chamani [27] in the hydraulics and fluid mechanics laboratory of the Civil Engineering Department at Isfahan University of Technology, Iran. As illustrated in Figure 4, the researchers conducted the experiments in an open rectangular glass flume with a length of 11 m, a width of 0.405 m, and a height of 1.2 m. The flume was horizontal, and the bed was raised 0.2 m for 5.1 m along the flume length. Moreover, 1.1 m of this region was filled with sand (study region), with a mean sediment diameter of 0.72 mm and a specific gravity of 2.65 g/cm^3. The remainder of this region (4 m) was raised by two metal platforms for 3 m (upstream platform) and 1 m (downstream platform). The cylindrical pier had a 40 mm diameter and was made of Teflon Plastic.

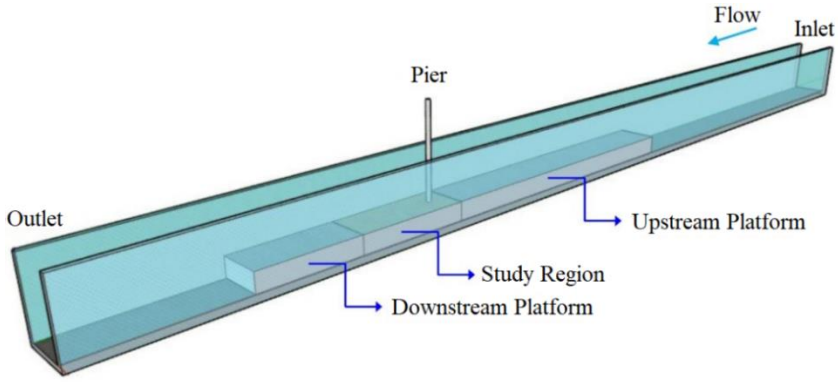

Figure 4. The experimental model in the study by Balouchi and Chamani (2012) [27]

2.3.2. *FLOW-3D* Model Setup and Calibration

Before running the model for different scenarios, it had to be calibrated. Similar to the experimental model, the numerical model was set up in *FLOW-3D*, as illustrated in Figure 5, for a flow rate of 45 L/s, an upstream water height of 0.2 m (on the platform), and a velocity of 0.56 m/s. The water was assumed to be clear and the bed uniform and sandy. Table 2 shows the mechanical properties of the sediment used in this study. The values presented in the table were obtained in the model calibration process. A total number of 1,100,000 mesh cells were used in the entire model; in order to obtain accurate results, near the pier, the dimensions of the grid cells were smaller than in other parts of the model. The grid size in the scour test area was 0.6 cm, while in other parts of the model it was 1 cm (Figure 5). These values were determined based on a trial and error procedure so that the simulation results matched the experimental results.

The maximum analysis time to reach equilibrium conditions was considered 25,200 s (420 min). The boundary conditions considered in the simulations were: Volume Flow Rate (VFR), used for the inflow; outflow, used for the water exiting the flume; wall, used for the sides and the bottom of the flume; and symmetry, used for the top of the flume, which assumes that all fluxes into this boundary are zero, and there is no friction (Figure 6). Furthermore, due to flow turbulence around the pier, the renormalized group (RNG) model was employed for the turbulence calculations [28]. There are, of course, other turbulence models to resolve a turbulent flow field. In particular, the use of the large eddy simulation (LES) technique may offer better results. On the other hand, longer computational time is needed in the use of LES [29]. In the present study, a less complicated turbulence model was employed to get an acceptable result in shorter time.

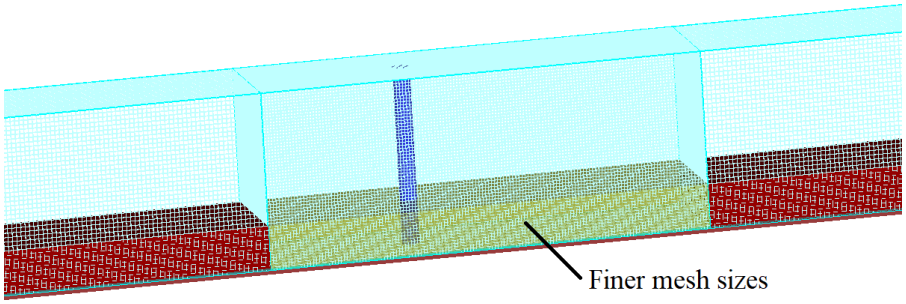

Figure 5. The meshing of the model

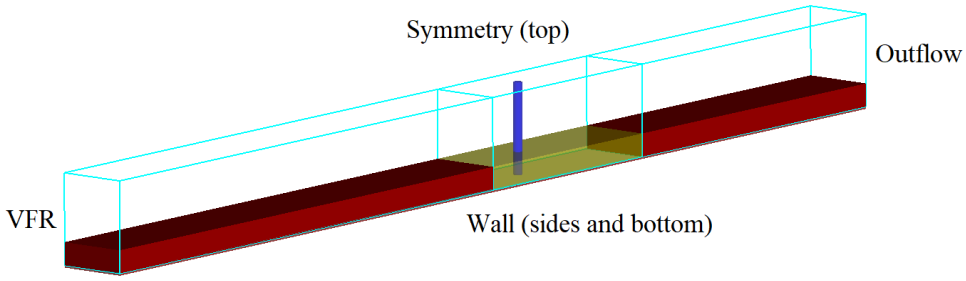

Figure 6. Model boundary conditions

The Nash–Sutcliffe (NS) model efficiency coefficient (Equation 12) was used to evaluate the model calibration.

$$NS = 1 - \frac{\sum_i |Q_m - Q_s|_i^2}{\sum_i |Q_{m,i} - \bar{Q}_m|_i^2} \quad (12)$$

Table 2. Mechanical properties of the sediment

Diameter (m)	Density (kg/m^3)	Drag coefficient	Entrainment coefficient	Bed load coefficient	The angle of repose (degrees)	Maximum packing fraction
72*10^{-5}	2,650	0.5	0.018	8	45	0.64

Where "Q" is a variable such as scour depth; measured and simulated are represented by "m" and "s," respectively; the bar indicates the average; and the ith measured or simulated value is "i". The NS function has a range of $-\infty$ to 1. NS = 1 means there is a perfect match between the simulated values and the observed data. The values between 0 and 1 show that the simulated values and observed data are relatively close to each other, whereas values less than 0 indicate that the model has no predictive power [30].

A comparison between the scour depths in the experimental and numerical model (Figure 7), in the front and back of the pier, during 25,200 s of operation indicated that the results match perfectly. The NS values obtained were 0.98 and 0.97, for the front and back of the pier, respectively. Moreover, after 20 minutes, both curves leveled off and the maximum scour depths at the end of both the experiment and simulation were very close to the values at 20 minutes.

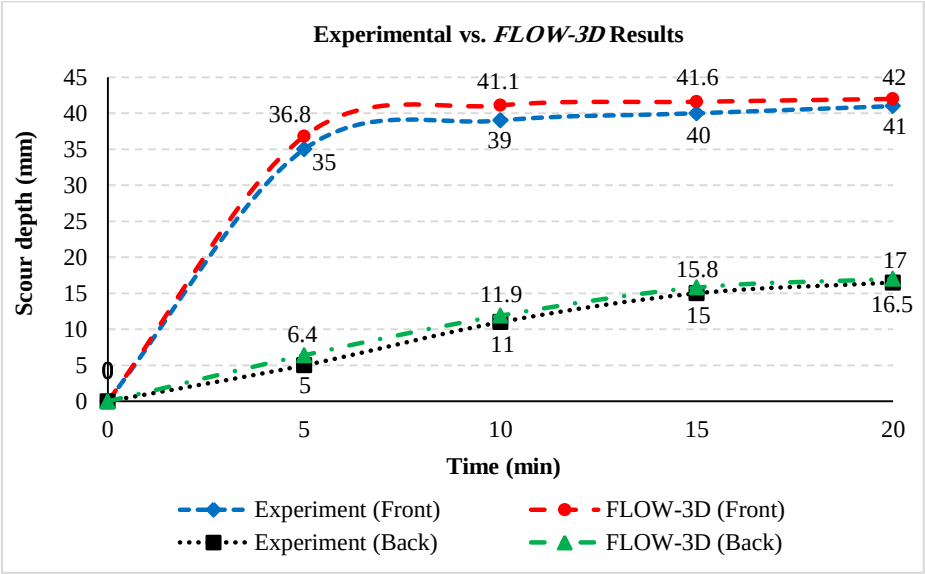

Figure 7. Comparison between scour depth in the experimental model and the numerical model

2.3.3. Scenarios

In this study, to investigate scouring around a bridge pier, while implementing sacrificial piles in front of the pier as a countermeasure against scouring, nine scenarios of the sacrificial pile arrangements were considered, based on the ease of construction and the engineering judgment of the authors. These scenarios are presented in Table 3 and Figure 8. In all scenarios, the pier diameter was 4 cm and pile diameters were 2 cm.

Table 3. Arrangements of sacrificial piles in different scenarios

Scenario	Number of sacrificial piles	Distance from the pier
S-1	0	-
S-2	1	4 times the pier diameter
S-3	1	5 times the pier diameter
S-4	1	6 times the pier diameter
S-5	3	2 and 3 times the pier diameter
S-6	3	3 and 5 times the pier diameter
S-7	3	4 and 6 times the pier diameter
S-8	5	2, 4 and 6 times the pier diameter
S-9	5	4, 6 and 8 times the pier diameter

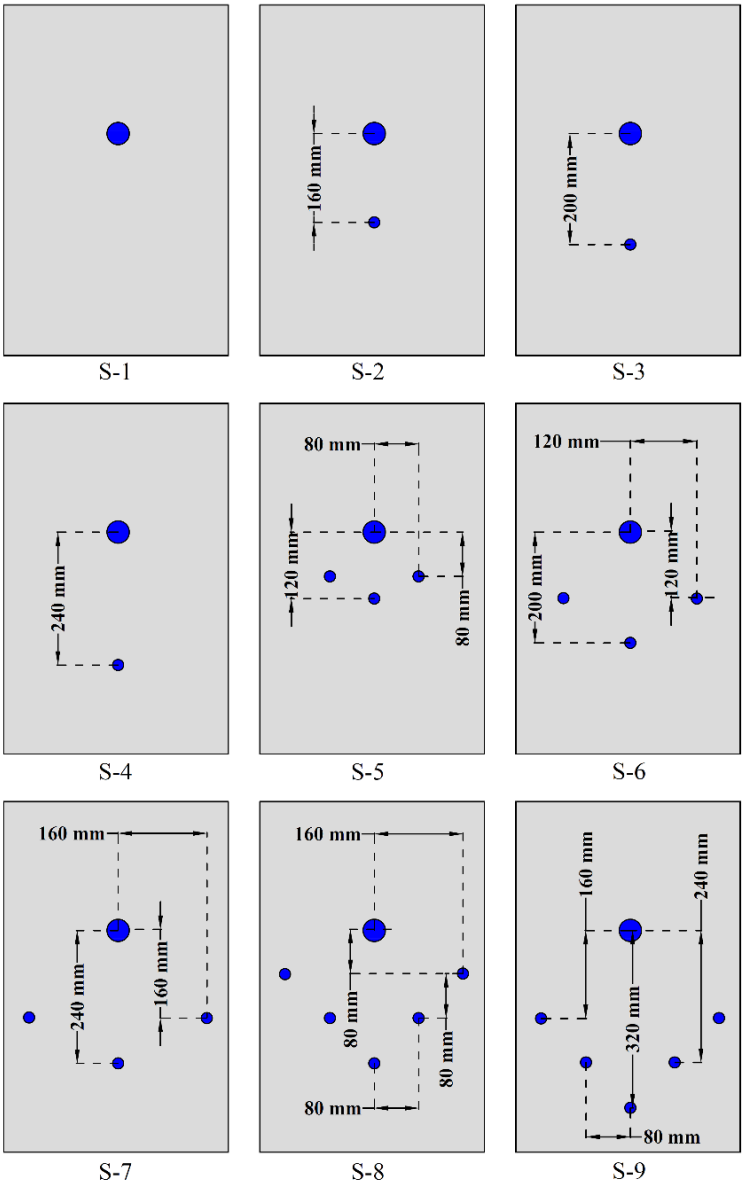

Figure 8. Different arrangements of the sacrificial piles

3. Results and Discussion

The simulation results showed that the development of the scour depth initially occurred at a faster rate, and over time, approached a state of equilibrium. In all simulations, almost 60% of total scouring occurred in less than 0.1 of the time required for the model to reach an equilibrium. The simulation results for all scenarios are shown in Figure 9. Moreover, Figure 10 summarizes the scour depths in the front, back, and sides of the pier.

The results show that the effectiveness of implementing sacrificial piles as scour countermeasures is dependent on the arrangement of the piles, which impacts horseshoe vortex formation, and ultimately, scour depth. Among all scenarios, except for S-1, in which no piles were installed in front of the pier, the maximum scour depth in front of the pier was observed under S-4 (32.3 mm). In this scenario, one single pile was placed in front of the pile at a distance of six times the pier diameter. On the other hand, the minimum scour depth in front of the pier was observed under S-5 and S-8 (19.6 mm). In these scenarios, a group of piles was installed upstream of the pier.

Regarding the scour depth in the back of the pier, the maximum was observed under S-3 and S-4. In these scenarios, a single pile was installed upstream of the pier at five and six times the pier diameter. On the other hand, the minimum was observed under S-8. In this scenario, five piles were installed upstream of the pier, at two, four, and six times the pier diameter.

Based on the results, whether using a single pile or a group of piles upstream of the pier, as the pile locations were closer to the pier, the scour depths in the front and back of the pier were lower.

In all scenarios, the scour depth in front of the pier was greater than in the back, with the ratio of the scour depth in the front to the back of the pier between 1.72 (S-5: using three piles upstream of the pier, located at two and three times the pier diameter) and 2.54 (S-4: using one pile upstream of the pier, located at six times the pier diameter).

Moreover, the maximum scour depth on the sides of the pier was observed in S-7 (44 mm). In this scenario, three piles were installed upstream of the pier, located at four and six times the pier diameter. On the other hand, the minimum scour depth on the sides of the pier was observed in S-8 (21 mm). The results show that, similar to the scour depth in front and in the back of the pier, installing the piles closer to the pier decreased the scour depth on the sides of the pier.

Comparing the scour depths in S-2 to S-9, with S-1 (not using any piles), it can be concluded that the application of sacrificial piles is an effective countermeasure to reduce the scour depth around piers in river bridges. The reason can be attributed to the formation of a lower-velocity region between the pier and the sacrificial piles, which reduces the scour depth.

The results of this study are in accordance with the findings of Abdeldayem et al. [10]. They investigated the effect of installing different configurations of a group of square sacrificial piles in front of a bridge pier, as a countermeasure against scouring. The authors reported that the method was effective in reducing the scour depth. Similarly, Melville and Hadfield reported that sacrificial piles can reduce the scour depth, as far as flow remains aligned, and the flow intensity is relatively small [12].

Regarding the cost of construction and maintenance, in cases where more piles are used upstream of the pier, the costs are higher and more accuracy in engineering design is required. However, the use of a single pile, despite the small difference in scour depth compared to other arrangements, is more economical than using several piles. Considering factors such as design convenience, low construction and maintenance costs, as well as an almost 70% reduction in scour depth around the bridge pier, S-3 (using a single pile, installed upstream of the pier, at a distance of five times the pier diameter) is recommended as the most efficient countermeasure against scouring in bridge piers, among the scenarios studied.

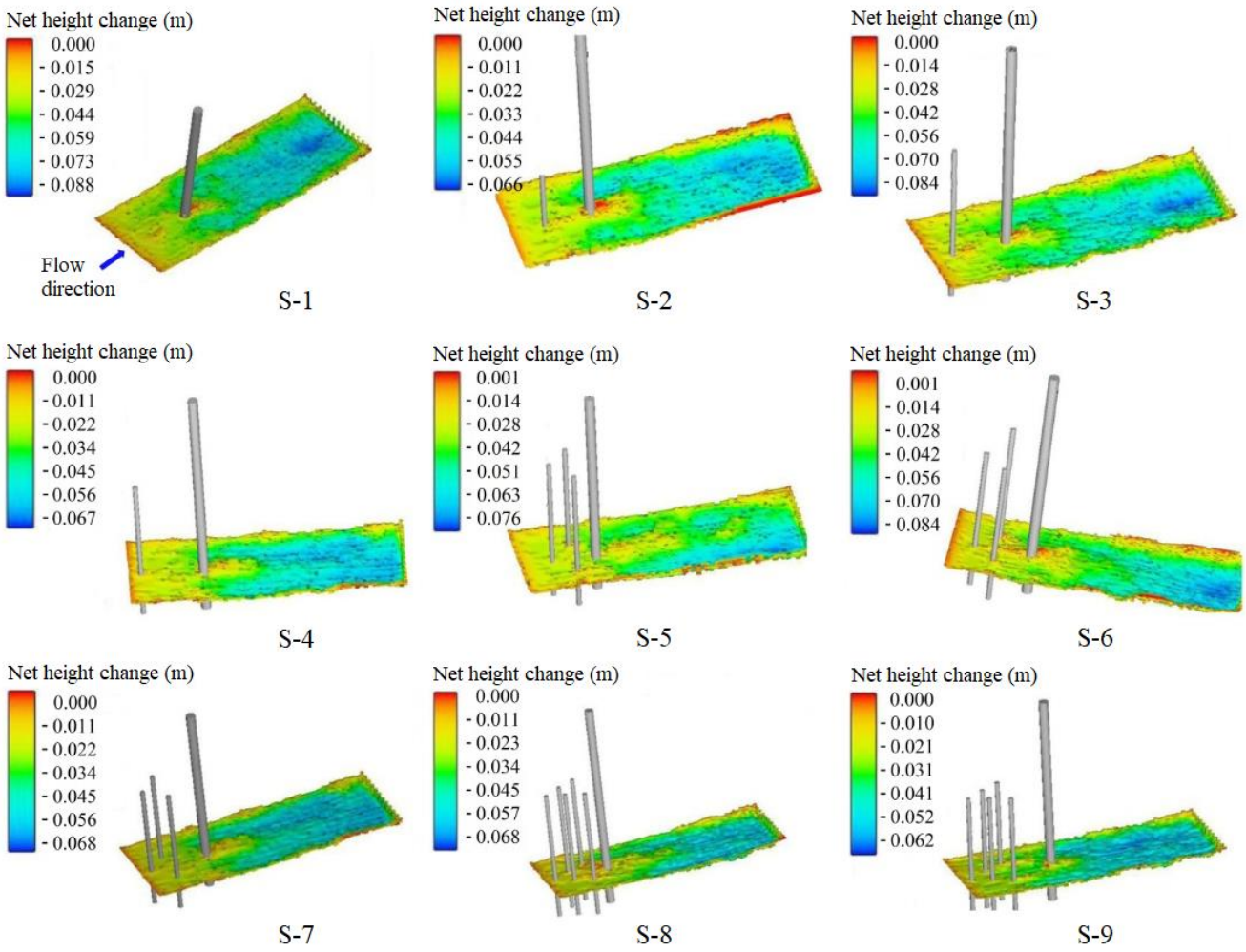

Figure 9. Simulation results (packed sediment height net change) after the steady-state

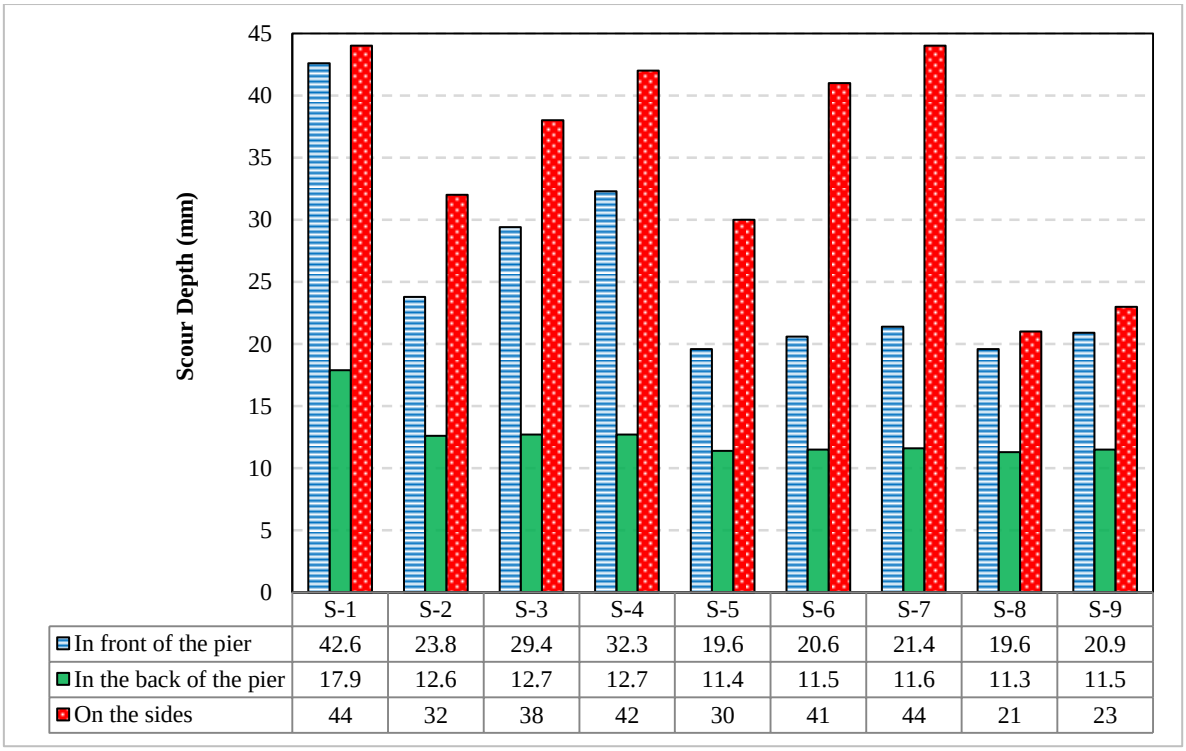

	S-1	S-2	S-3	S-4	S-5	S-6	S-7	S-8	S-9
In front of the pier	42.6	23.8	29.4	32.3	19.6	20.6	21.4	19.6	20.9
In the back of the pier	17.9	12.6	12.7	12.7	11.4	11.5	11.6	11.3	11.5
On the sides	44	32	38	42	30	41	44	21	23

Figure 10. Scour depth in different scenarios

4. Conclusions

Since scouring around bridge foundations in rivers and estuaries is a major cause of bridge failure, estimation of the maximum scour depth is of great importance to engineers. In this study, the *FLOW-3D* model Ver. 11.2 was employed to simulate scouring around a bridge pier in clear-water conditions with a uniform sandy bed. The numerical model was calibrated based on an experimental study by Balouchi and Chamani [27]. Using the calibrated model, nine novel scenarios with different sacrificial pile arrangements as countermeasures against scouring were studied. The following summarizes the main findings of this study:

- The effectiveness of using sacrificial piles as scour countermeasures is dependent on their arrangement, which impacts horseshoe vortex formation, and ultimately the scour depth around the pier;
- The scour depths initially developed at a faster rate, and approached a state of equilibrium over time;
- In all scenarios, almost 60% of scouring occurred in less than 0.1 of the time required for the model to reach an equilibrium;
- The maximum scour depth in front of the pier was observed under S-4 (32.3 mm). In this scenario, one single pile was placed upstream of the pile at a distance of six times the pier diameter;
- The minimum scour depth in front of the pier was observed under S-5 and S-8 (19.6 mm). In these scenarios, a group of piles were installed upstream of the pier;
- The maximum scour depth in the back of the pier was observed under S-3 and S-4. In these scenarios, a single pile was installed upstream of the pier at five and six times the pier diameter;
- The minimum scour depth in the back of the pier was observed under S-8. In this scenario, five piles were installed upstream of the pier, at two, four, and six times the pier diameter;
- The maximum scour depth on the sides of the pier was observed in S-7 (44 mm). In this scenario, three piles were installed upstream of the pier, located at four and six times the pier diameter;
- The minimum scour depth on the sides of the pier was observed in S-8 (21 mm).

The results showed that using sacrificial piles significantly reduced the scour depths. Comparing the simulation results, maximum scouring occurred on the sides of the pier in all scenarios. In addition, minimum scouring occurred when there were a greater number of sacrificial piles installed closer to the bridge pier. In all scenarios, the scour depth in front of the pier was greater than in the back, with the ratio of the scour depth in the front to the back of the pier between 1.72 (S-5) and 2.54 (S-4).

In this study, a non-sticky uniform sediment layer was used. In the future studies, the impact of several layers of sticky and non-sticky sediments on scouring can be investigated; Moreover, similar simulations can be performed using different turbulence models and different Froude numbers. Finally, this study was performed on a circular pier. In future studies, different shapes of bridge piers can be investigated while using sacrificial piles as countermeasures against scouring.

5. Conflicts of Interest

The authors declare no conflict of interest.

6. References

[1] Karakouzian, Chavez, Hayes, and Nazari-Sharabian. “Bulbous Pier: An Alternative to Bridge Pier Extensions as a Countermeasure Against Bridge Deck Splashing.” Fluids 4, no. 3 (July 24, 2019): 140. doi:10.3390/fluids4030140.

[2] Karami, Mehrdad, Abdorreza Kabiri-Samani, Mohammad Nazari-Sharabian, and Moses Karakouzian. “Investigating the Effects of Transient Flow in Concrete-Lined Pressure Tunnels, and Developing a New Analytical Formula for Pressure Wave Velocity.” Tunnelling and Underground Space Technology 91 (September 2019): 102992. doi:10.1016/j.tust.2019.102992.

[3] Karakouzian, Moses, Mohammad Nazari-Sharabian, and Mehrdad Karami. “Effect of Overburden Height on Hydraulic Fracturing of Concrete-Lined Pressure Tunnels Excavated in Intact Rock: A Numerical Study.” Fluids 4, no. 2 (June 19, 2019): 112. doi:10.3390/fluids4020112.

[4] Chiew, Yee-Meng. "Scour protection at bridge piers." Journal of Hydraulic Engineering 118, no. 9 (1992): 1260-1269. doi:10.1061/(ASCE)0733-9429(1992)118:9(1260).

[5] Shen, Hsieh Wen, Verne R. Schneider, and Susumu Karaki. "Local scour around bridge piers." Journal of the Hydraulics Division (1969): 1919-1940.

[6] Richardson, E.V., and Davis, S.R. “Evaluating Scour at Bridges”. Hydraulic Engineering Circular. (2001), 18 (HEC-18), Report no. FHWA NHI 01–001, U.S. Department of Transportation, Federal Highway Administration, Washington, DC, USA.

[7] Elsaeed, Gamal, Hossam Elsersawy, and Mohammad Ibrahim. “Scour Evaluation for the Nile River Bends on Rosetta Branch.” Advances in Research 5, no. 2 (January 10, 2015): 1–15. doi:10.9734/air/2015/17380.

[8] Chang, Wen-Yi, Jihn-Sung Lai, and Chin-Lien Yen. "Evolution of scour depth at circular bridge piers." Journal of Hydraulic Engineering 130, no. 9 (2004): 905-913. doi:10.1061/(ASCE)0733-9429(2004)130:9(905).

[9] Unger, Jens, and Willi H. Hager. "Riprap failure at circular bridge piers." Journal of Hydraulic Engineering 132, no. 4 (2006): 354-362. doi:10.1061/(ASCE)0733-9429(2006)132:4(354).

[10] Abdeldayem, Ahmed W., Gamal H. Elsaeed, and Ahmed A. Ghareeb. "The effect of pile group arrangements on local scour using numerical models." Advances in Natural and Applied Sciences 5, no. 2 (2011): 141-146.

[11] Sheppard, D. M., B. Melville, and H. Demir. “Evaluation of Existing Equations for Local Scour at Bridge Piers.” Journal of Hydraulic Engineering 140, no. 1 (January 2014): 14–23. doi:10.1061/(asce)hy.1943-7900.0000800.

[12] Melville, Bruce W., and Anna C. Hadfield. "Use of sacrificial piles as pier scour countermeasures." Journal of Hydraulic Engineering 125, no. 11 (1999): 1221-1224. doi:10.1061/(ASCE)0733-9429(1999)125:11(1221).

[13] Yao, Weidong, Hongwei An, Scott Draper, Liang Cheng, and John M. Harris. “Experimental Investigation of Local Scour Around Submerged Piles in Steady Current.” Coastal Engineering 142 (December 2018): 27–41. doi:10.1016/j.coastaleng.2018.08.015.

[14] Link, Oscar, Marcelo García, Alonso Pizarro, Hernán Alcayaga, and Sebastián Palma. “Local Scour and Sediment Deposition at Bridge Piers During Floods.” Journal of Hydraulic Engineering 146, no. 3 (March 2020): 04020003. doi:10.1061/(asce)hy.1943-7900.0001696.

[15] Khan, Mujahid, Mohammad Tufail, Muhammad Fahad, Hazi Muhammad Azmathullah, Muhammad Sagheer Aslam, Fayaz Ahmad Khan, and Asif Khan. "Experimental analysis of bridge pier scour pattern." Journal of Engineering and Applied Sciences 36, no. 1 (2017): 1-12.

[16] Yang, Yifan, Bruce W. Melville, D. M. Sheppard, and Asaad Y. Shamseldin. “Clear-Water Local Scour at Skewed Complex Bridge Piers.” Journal of Hydraulic Engineering 144, no. 6 (June 2018): 04018019. doi:10.1061/(asce)hy.1943-7900.0001458.

[17] Moussa, Yasser Abdallah Mohamed, Tarek Hemdan Nasr-Allah, and Amera Abd-Elhasseb. “Studying the Effect of Partial Blockage on Multi-Vents Bridge Pier Scour Experimentally and Numerically.” Ain Shams Engineering Journal 9, no. 4 (December 2018): 1439–1450. doi:10.1016/j.asej.2016.09.010.

[18] Guan, Dawei, Yee-Meng Chiew, Maoxing Wei, and Shih-Chun Hsieh. “Characterization of Horseshoe Vortex in a Developing Scour Hole at a Cylindrical Bridge Pier.” International Journal of Sediment Research 34, no. 2 (April 2019): 118–124. doi:10.1016/j.ijsrc.2018.07.001.

[19] Dougherty, E.M. "CFD Analysis of Bridge Pier Geometry on Local Scour Potential" (2019). LSU Master's Theses. 5031.

[20] Vijayasree, B. A., T. I. Eldho, B. S. Mazumder, and N. Ahmad. “Influence of Bridge Pier Shape on Flow Field and Scour Geometry.” International Journal of River Basin Management 17, no. 1 (November 10, 2017): 109–129. doi:10.1080/15715124.2017.1394315.

[21] Farooq, Rashid, and Abdul Razzaq Ghumman. “Impact Assessment of Pier Shape and Modifications on Scouring Around Bridge Pier.” Water 11, no. 9 (August 23, 2019): 1761. doi:10.3390/w11091761.

[22] Link, Oscar, Cristian Castillo, Alonso Pizarro, Alejandro Rojas, Bernd Ettmer, Cristián Escauriaza, and Salvatore Manfreda. “A Model of Bridge Pier Scour During Flood Waves.” Journal of Hydraulic Research 55, no. 3 (November 18, 2016): 310–323. doi:10.1080/00221686.2016.1252802.

[23] Karakouzian, Moses, Mehrdad Karami, Mohammad Nazari-Sharabian, and Sajjad Ahmad. “Flow-Induced Stresses and Displacements in Jointed Concrete Pipes Installed by Pipe Jacking Method.” Fluids 4, no. 1 (February 21, 2019): 34. doi:10.3390/fluids4010034.

[24] Flow Science, Inc. FLOW-3D User’s Manual, Flow Science (2018).

[25] Brethour, J. Modeling Sediment Scour. Flow Science, Santa Fe, NM. (2003).

[26] Brethour, James, and Jeff Burnham. "Modeling sediment erosion and deposition with the FLOW-3D sedimentation & scour model." Flow Science Technical Note, FSI-10-TN85 (2010): 1-22.

[27] Balouchi, M., and Chamani, M.R. “Investigating the Effect of using a Collar around a Bridge Pier, on the Shape of the Scour Hole”. Proceedings of the First International Conference on Dams and Hydropower (2012) (In Persian).

[28] Bayon, Arnau, Daniel Valero, Rafael García-Bartual, Francisco José Vallés-Morán, and P. Amparo López-Jiménez. “Performance Assessment of OpenFOAM and FLOW-3D in the Numerical Modeling of a Low Reynolds Number Hydraulic Jump.” Environmental Modelling & Software 80 (June 2016): 322–335. doi:10.1016/j.envsoft.2016.02.018.

[29] Aminoroayaie Yamini, O., S. Hooman Mousavi, M. R. Kavianpour, and Azin Movahedi. “Numerical Modeling of Sediment Scouring Phenomenon Around the Offshore Wind Turbine Pile in Marine Environment.” Environmental Earth Sciences 77, no. 23 (November 24, 2018). doi:10.1007/s12665-018-7967-4.

[30] Nazari-Sharabian, Mohammad, Masoud Taheriyoun, Sajjad Ahmad, Moses Karakouzian, and Azadeh Ahmadi. “Water Quality Modeling of Mahabad Dam Watershed–Reservoir System under Climate Change Conditions, Using SWAT and System Dynamics.” Water 11, no. 2 (February 24, 2019): 394. doi:10.3390/w11020394.